The chlorination of *N*-methyl amino acids with hypochlorous acid: kinetics and mechanisms

Fruzsina Simon[a], *Eszter Kiss*[a], *Mária Szabó*[a,]*, *István Fábián*[a,b]*

a: Department of Inorganic and Analytical Chemistry, University of Debrecen, Egyetem tér 1, 4032 Debrecen, Hungary

b: MTA-DE Redox and Homogeneous Catalytic Reaction Mechanisms Research Group, University of Debrecen, Egyetem tér 1, 4032 Debrecen, Hungary

* Corresponding authors: Mária Szabó: szabo.maria@science.unideb.hu

István Fábián: ifabian@science.unideb.hu

KEYWORDS

N-methyl amino acid, hypochlorous acid, chlorination, kinetics and mechanism, Schiff base

ABSTRACT

The formation and decomposition kinetics of *N*-chloro-*N*-methyl amino acids were studied to predict the fate and impact of these compounds in water treatment technologies and biological systems. These compounds form in fast second order reactions between *N*-methyl amino acids and hypochlorous acid. The comparison of the activation parameters for the reactions of *N*-methyl substituted and non-substituted branched chain amino acids reveals the transition state features less organized structure and stronger bonds between the reactants in the reactions with the *N*-methyl derivatives. This is due to a combined positive inductive effect of the *N*-methyl group and the alkyl sidechain, as well as to the steric effects of the substituents. *N*-methyl-*N*-chloro amino acids decompose much faster than the non-substituted compounds. The reaction rates do not depend on the pH and the same final product is formed in the entire pH range. *N*-chlorosarcosine is an exception, it decomposes via competing paths, $k_d^{obs} = k_d + k_d^{OH}[OH^-]$, yielding different final products. This feature is most likely due to the lack of an alkyl substituent on the α-carbon atom. Under physiological pH, aldehydes and methylamine form in these reactions which are not particularly toxic.

INTRODUCTION

The formation of chlorinated disinfection byproducts (DBP) is of primary concern in water treatment technologies.[1-3] Amino acids, their derivatives and related compounds are among the most common contaminants in raw and swimming pool waters. Thus, environmental and biological relevance has generated immense interest in the reactions of hypochlorous acid (HOCl) with amino acids. In chlorination water treatment technologies, the oxidant is typically used in excess and predominantly *N*,*N*-dichloro compounds are formed, however, depending on the actual conditions (pH, the dosage of HOCl, temperature etc.) *N*-chloro amino acids are also produced as intermediates or byproducts.[4, 5] These compounds are considered as secondary disinfectants which are less efficient than HOCl but last longer in water supply systems.[6] Their decomposition may lead to the formation of antagonistic intermediates and final products. For example, the formation of aldehydes from *N*-chloro amino acids may induce taste and odor issues in drinking water.[7-9]

The very same reactions are also important in biological systems. During inflammatory processes, hydrogen-peroxide oxidizes chloride ion to HOCl in a myeloperoxidase enzyme catalyzed process.[10-12] In turn, HOCl plays a pivotal role in the defense mechanism against invading pathogens. Apart from reacting with peptides and proteins, it chlorinates free available amino acids. The product *N*-chloro amino acids penetrate into the cells and cause oxidative stress which leads to necrosis or apoptosis.[13-21] Since amino compounds are abundant in living organisms, *in vivo* formation of *N*,*N*-dichloro amines can be excluded.

In recent studies, we have investigated the formation and decomposition kinetics and mechanisms of several *N*-chloro amino acids and the decomposition of mono-chloramine.[7, 22-25] It was confirmed that the functional group on the α-carbon atom significantly influences the kinetics of the decomposition and these reactions exhibit distinct mechanistic features. It was

shown that *N*-chloroglycine decomposes in a hydroxide ion catalyzed process and the intermediates as well as the final product of the reaction may have significant biological activities.[23] Thus, *N*-oxalylglycine was identified as a key intermediate which is an efficient demethylase inhibitor.[26-28] The final product of the reaction is *N*-formylglycine which is capable to influence sulfatase enzyme activities.[29-32] The decomposition of *N*-chloroalanine proceeds via two competing reaction paths and the kinetics and stoichiometry of the overall process are controlled by the pH. The sole product of the neutral path is acetaldehyde while the hydroxide ion catalyzed process yields pyruvate ion and *N*-acetylalanine as major and minor products, respectively.[24] The decomposition of *N*-chloro-BCAAs (branched chain amino acids) also occurs via competing spontaneous and hydroxide ion catalyzed reaction paths. However, regardless of the pH, the final product is always the corresponding aldehyde formed via decarboxylation and subsequent deamination of the parent compounds.[7] In the absence of the bulky alkyl substituents on the α-carbon atom, these steps occur in reverse order under alkaline conditions and yield different products as shown in the case of *N*-chloroglycine and *N*-chloro-α-alanine.

In a recent study, Zhao et.al reported a detailed computational study on the decomposition of several *N*-chloro amino acids emphasizing the need for solid experimental data to explore how the substituents affect the degradation mechanisms in these systems.[33] Considering the noted kinetic role of the α-alkyl substituents in the decomposition of *N*-chloro amino acids, it is an intriguing issue how direct alkyl substitution of the amino group affects these reactions. *N*-methyl amino acids also exist in living systems and in water resources. Most prominently, *N*-methylglycine (sarcosine) is part of the metabolic pathway of choline. This pathway involves the conversion of choline into glycine via sarcosine which forms as an intermediate from *N*,*N*-dimethylglycine in a dimethylglycine dehydrogenase enzyme catalyzed process.[34] Sarcosinaemia is a well-known, but rare inborn error of amino acid metabolism characterized by the elevated

concentration of sarcosine in plasma and urine.[35, 36] The cause of this disease is the malfunction of the sarcosine dehydrogenase enzyme or the electron transport flavoprotein.[37] Sreekumar et al. identified sarcosine as a differential metabolite that was highly increased during prostate cancer progression to metastasis and could be detected non-invasively in urine.[38]

The main goals of this study are to provide detailed mechanistic insight into the reactions of HOCl with *N*-methyl substituted amino acids, to identify the products and to compare the results with those obtained with the corresponding non-substituted compounds. Most importantly, it needs to be clarified how stable the chlorinated *N*-methyl compounds are and whether their decomposition reactions generate toxic or biologically active products and by-products. Earlier, Armesto et al. discussed possible mechanisms for the decomposition of *N*-chloro-*N*-methylglycine and –alanine on the basis of experimental data obtained under somewhat limited experimental conditions. Most importantly, the pH dependence of the decomposition was not studied in detail, and possible side reactions with the products were not considered.[10, 39] Now we report an exhaustive study on the formation and decomposition kinetics of five *N*-chloro-*N*-methyl amino acids. We provide in-depth analysis of the kinetic role of the alkyl substituents in these compounds and propose a detailed mechanism which explains all the experimental observations in these systems. The results are relevant in water treatment technologies and also contribute to better understanding of the molecular background of vital *in vivo* processes.

MATERIALS AND METHODS

Materials

Chloride ion free sodium hypochlorite solution was prepared as described earlier.[40, 41] The stock solution of NaOCl was stored at 4 °C in the dark and its concentration was determined before use as described earlier.[22, 24]

N-methylglycine (NMG), *N*-methyl-*L*-alanine (NMA), *N*-methyl-*L*-valine (NMV), *N*-methyl-*L*-leucine × 2HCl (NML), *N*-methyl-*L*-isoleucine (NMI), acetaldehyde (Aca), iso-valeraldehyde (Iva), 2-methyl-butyraldehyde (Mba), isobutyraldehyde (Iba), methylamine (MA) and glyoxalic acid (Sigma-Aldrich) and all other chemicals were of reagent grade. The samples were prepared in doubly deionized and ultrafiltered water from a Purelab Classic (ELGA) water purification system. The kinetic measurements were made at 25.0 ± 0.1 °C and 1.0 M ionic strength set with $NaClO_4$ prepared from $HClO_4$ and NaOH (Sigma-Aldrich).[42] The pH was adjusted using Na_2HPO_4/NaH_2PO_4 and $Na_2B_4O_7$ buffers or NaOH solution under alkaline conditions.

Instruments and Methods

Iodometric and pH-metric titrations were made with a Metrohm 888 Titrando system equipped with Metrohm 6.0451.100 combination platinum and Metrohm 6.0262.100 combination glass electrodes, respectively. The readout of the pH meter was converted to $pH = -\log[H^+]$ thorough this paper.[43] The acid dissociation constants of the *N*-methyl amino acids were determined on the basis of pH-metric titrations by evaluating the data with the dedicated program, SUPERQUAD.[44]

The formation kinetics of the *N*-chloro compounds was monitored with an Applied Photophysics SX-20 stopped-flow instrument. Kinetic traces were obtained as the average of 3 – 5 runs.

The decomposition of the *N*-chloro compounds was monitored with an Agilent Technologies Cary 8454 UV – VIS diode array spectrophotometer. It was confirmed that photochemical interference by the spectrophotometer did not occur.[45] The temperature of the cell was controlled by the built-in thermoelectric Peltier device. The baseline was recorded with solutions containing the excess amino acid. Kinetic experiments were performed by mixing the appropriate substrate and hypochlorite ion solutions in stoppered tandem quartz cuvettes and monitoring the absorbance change over the 220 − 350 nm spectral range.

The first-order kinetic traces were fitted with the controlling software of the stopped-flow instrument. Other data fitting was made with the program package OriginPro 2018 using nonlinear least-squares routines.[46]

All NMR measurements were made by using a Bruker DRX 400 (9.4 T) NMR spectrometer equipped with a Bruker VT-1000 thermo-controller and BB inverse z gradient probe (5 mm). Each solution was prepared in H_2O, and DSS (4,4-dimethyl-4-silapentane-1-sulfonic acid) in D_2O was added to the sample in a capillary as an external standard for ^1H (0.00 ppm (s), 0.63 ppm (t), 1.76 ppm (m) and 2.91 ppm (t)). The ^1H NMR spectra were recorded by using the standard Bruker watergate pulse sequence for suppressing the water proton signal. In each experiment, 32 scans were collected with 16K data points using a sweep width of 5995 Hz, a pulse angle of 90°, an acquisition time of 1.366 s, and a relaxation delay of 1 s.

RESULTS AND DISCUSSION

Formation kinetics of *N*-chloro-*N*-methyl amino acids

The chlorination of *N*-methyl amino acids with HOCl exhibits very similar features compared to the corresponding reactions of the non-substituted compounds.[22] In the excess of *N*-methyl amino acid over HOCl, simple first order kinetic traces were observed under alkaline conditions. The kinetic traces were fitted to a simple exponential function (Eq. (S1)), and the pseudo first order rate constants (k_{obs}^{1st}) are linearly dependent on the amino acid concentration (Figure S1, Supporting Information), and do not depend on the concentration of HOCl. Thus, the formation of the *N*-chloro-*N*-methyl amino acids (NCAA) is an overall second order reaction (Eq. (1)).

$$\frac{dc_{NCAA}}{dt} = k_{obs}^{2nd} c_{HOCl} c_{AA} \qquad (1)$$

where c_{HOCl} and c_{AA} are the total concentrations of hypochlorous acid and the *N*-methyl amino acid, respectively. [47]

The rate of *N*-chloro-*N*-methyl amino acid formation is strongly pH dependent. Under slightly alkaline conditions the reaction is very fast, and meaningful stopped-flow kinetic traces could be obtained only when the reactants were used in comparable concentrations. The corresponding second order rate constants (k_{obs}^{2nd}) were obtained by fitting the kinetic traces to the appropriate second-order expression (Eq. (S2)).

The rate constants exhibit a characteristic bell-shape pH dependence (Figure 1). This feature is interpreted in terms of the acid-base equilibria of the reactants. In agreement with earlier results, this observation confirms that the reactive species are the HOCl form of the oxidant and the fully deprotonated amino acid in these reactions. The rate constant is expressed by Eq. (2).[48]

$$k_{obs}^{2nd} = k \frac{K_{AA}[H^+]}{(K_{AA} + [H^+])(K_{HOCl} + [H^+])} \quad (2)$$

where k_{obs}^{2nd}, K_{AA} and K_{HOCl} are the pH dependent second order rate constant, the acid dissociation constants of the protonated amino group of the *N*-methyl amino acid and hypochlorous acid, respectively. The reaction proceeds at the highest rate when the pH is equal with the average of pK_{AA} and pK_{HOCl}.

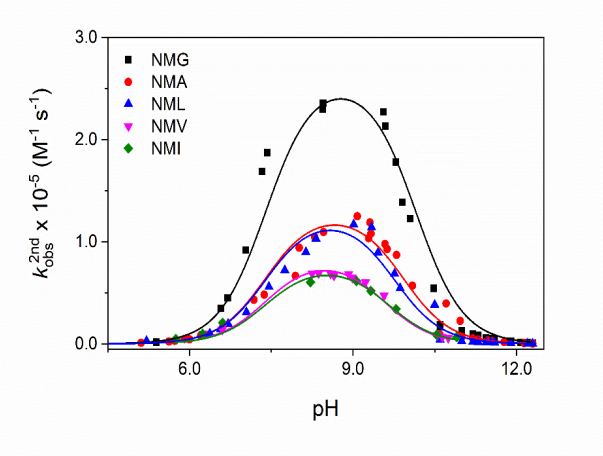

Figure 1. The pH dependence of k_{obs}^{2nd}. Experimental data (markers) and fitted curves according to Eq. (2) (solid lines). I = 1.00 M ($NaClO_4$), T = 25.0 °C.

The rate constants were estimated by fitting Eq. (2) to the experimental data. In these calculations, K_{AA} and K_{HOCl} were included with fixed values. The acid dissociation constants of the *N*-methyl amino acids were determined by pH-metric titrations in this work (Table 1) while the pK_a of HOCl was taken from our earlier study (pK_a = 7.40[40]).

The parameters of activations for the chlorination of *N*-methyl amino acids were estimated on the basis of temperature dependent studies under alkaline conditions in the 11 – 40 °C range. Under such conditions, K_{HOCl} and K_{AA} >> $[H^+]$, and Eq. (2) transforms into Eq. (3).

$$k_{obs}^{2nd} = k \frac{1}{[OH^-]} \frac{K_w}{K_{HOCl}} \quad (3)$$

where K_w is the water ionic product.

The temperature dependence of K_w, K_{AA} and k can be taken into account by using the van't Hoff and the Eyring-Polányi equations, respectively, and Eq. (3) can be rewritten as Eq. (4).

$$k_{obs}^{2nd} = \frac{k_B T}{h} e^{\frac{\Delta S^{\ddagger}}{R}} e^{-\frac{\Delta H^{\ddagger}}{RT}} \frac{1}{[OH^-]} \frac{e^{-\frac{\Delta H_w}{RT}} e^{\frac{\Delta S_w}{R}}}{e^{-\frac{\Delta H_{HOCl}}{RT}} e^{\frac{\Delta S_{HOCl}}{R}}} \quad (4)$$

The experimental data were fitted to Eq. (4) (Figure S2). The thermodynamic parameters for the acid base equilibria of the reactants were obtained from the literature and were kept fixed during the calculations: ΔH_w = 48.7 kJ mol^{-1} K^{-1}, ΔS_w = −97.8 J mol^{-1} K^{-1} [22], ΔH_{HOCl} = 12.4 kJ mol^{-1} K^{-1}, ΔS_{HOCl} = −99.7 J mol^{-1} K^{-1} [40]. The calculated activation enthalpies ($\Delta H^{\ddagger}$) and entropies ($\Delta S^{\ddagger}$) are listed in Table 1.

Table 1. The kinetic parameters for the N-chlorination of *N*-methyl amino acids and the corresponding α-amino acids.[22] I = 1.00 M ($NaClO_4$), T = 25.0 °C.

Amino acid	$k \times 10^{-7}$ ($M^{-1}s^{-1}$)	$\Delta S^{\ddagger}$ ($Jmol^{-1}K^{-1}$)	$\Delta H^{\ddagger}$ ($kJmol^{-1}$)	pK_{AA}
N-methylglycine	14.7 ± 0.4	−29.9 ± 1.0	18.8 ± 0.3	10.15 ±0.01
glycine	3.94	−36.8	18.1	9.42
N-methylalanine	4.29 ± 0.09	−33.3 ± 6.3	19.0 ± 2.0	9.92 ± 0.01
α-alanine	2.91	−37.1	18.4	9.60
N-methylleucine	2.89 ± 0.07	3.7 ± 1.7	31.2 ± 0.5	9.76 ± 0.01
leucine	2.90	−73.1	7.73	9.49
N-methylisoleucine	1.38 ± 0.06	-10.1 ± 2.8	27.8 ± 0.9	9.65 ± 0.05
isoleucine	2.65	-59.0	12.3	9.46
N-methylvaline	1.24 ± 0.02	-17.0 ± 2.8	26.1 ± 0.9	9.57 ± 0.01
valine	3.35	-60.0	12.1	9.41

N-methyl substitution of the studied amino acid does not affect significantly the reactivity of the amino group toward HOCl. The rate constants are invariably several times 10^7 $M^{-1}s^{-1}$ as it was also reported for the *N*-chlorination of proteinogenic amino acids.[22] Apparently, the positive inductive effect of the methyl group is offset by the presence of the bulky alkyl substituents on the *α*-carbon atom. The only exception is glycine where the *N*-methyl group significantly increases the basicity of the amino group which becomes more susceptible for a reaction with an electrophilic agent. This change manifests itself in an about 3.5 times increase in the corresponding chlorination rate constants.

Nevertheless, a close inspection of the results reveals that the alkyl sidechain influences the kinetics of these reactions to some extent. The effect of the *N*-methyl group is somewhat offset by the alkyl substituent on the *α*-carbon atom as demonstrated by the relatively small differences in the corresponding pK_{AA} values. In the case of *α*-alanine, the rate constants correlate with the

pK_{AA} of the *N*-methyl substituted and non-substituted compounds. The replacement of the *α*-methyl group with an isobutyl group (leucine) eliminates this correlation. The alkyl chain branches at the close vicinity of the reaction center in isoleucine and valine, and their *N*-methyl substituted derivatives are less reactive by about a factor of 2 and 2.7 than the parent compounds, respectively. It is reasonable to assume that the attack of HOCl is somewhat sterically hindered by the alkyl groups and this effect depends on the bulkiness of the sidechain on the *α*-carbon atom.

In our recent study, it was concluded that $\Delta S^{\ddagger}$ becomes more negative and $\Delta H^{\ddagger}$ becomes smaller in the chlorination reactions of amino acids due to the presence of bulky substituents on the *α*-carbon atom.[22] Quite the opposite trend prevails in the reactions of the *N*-methyl substituted compounds. Compared to the chlorination of *N*-methylglycine and *α*-alanine, the parameters of activation are consistent with stronger bonds and less organized structures in the transition states of the reactions of *N*-methyl branched-chain amino acids. This phenomenon is probably the consequence of an HOCl induced combined positive inductive effect by the *N*-methyl group and the alkyl sidechain, and the steric effects of the substituents in the activated complex.

The decomposition of alkyl substituted *N*-chloro-*N*-methyl amino acids

The relatively slow decomposition of *N*-chloro α-amino acids occurs on a time scale of 2 – 4 hours.[7, 23, 24] The corresponding reactions of *N*-chloro-*N*-methyl amino acids exhibit remarkably different kinetic features as they proceed about two orders of magnitude faster at least. To some extent, it is unexpected because considerably smaller differences were reported for the decomposition of the derivatives of glycine and *α*-alanine in an earlier paper.[39] In the case of NCMA (*N*-chloro-*N*-methyl-*α*-alanine), NCML (*N*-chloro-*N*-methylleucine), NCMI (*N*-chloro-*N*-methylisoleucine) and NCMV (*N*-chloro-*N*-methylvaline), the time resolved spectral changes confirm very similar kinetic behavior in the entire neutral – alkaline pH range. (The

decomposition of NCMG (*N*-chlorosarcosine) deviates from the general kinetic pattern and will be discussed in subsequent part of this paper.) As an example, the decomposition of NCMA is shown in Figure 2.

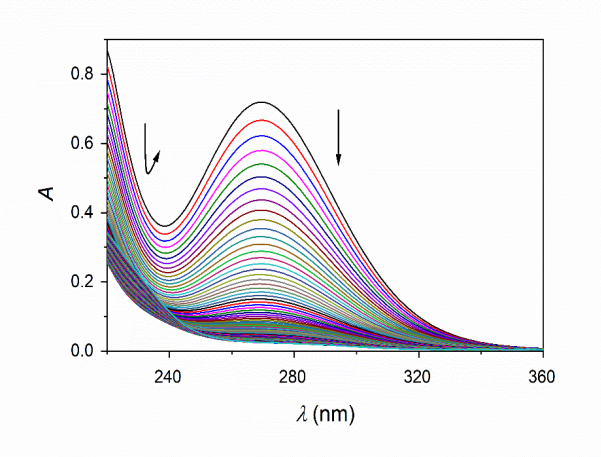

Figure 2. Time resolved spectral changes during the decomposition of NCMA under alkaline conditions. c_{NMA}^{0}= 3.00 × 10^{-3} M, c_{NCMA}^{0} = 3.00 × 10^{-3} M, [OH^-] = 5.00 × 10^{-2} M, I = 1.00 M ($NaClO_4$), T = 25.0 °C, Δt = 5 s, t =1000 s.

The absorbance decay at the characteristic absorbance band of NCMA (λ_{max} ~ 270 nm) is consistent with first-order kinetics and the corresponding rate constant, k_d, was obtained by fitting the kinetic traces to the appropriate rate expression. The absorbance change at lower wavelengths exhibits a relatively slow increase after the initial decay. This observation is consistent with a subsequent reaction of a product (Figure S3). The decomposition of the *N*-chloro-*N*-methyl-BCAAs also occurs in a first order process, however, the second step was not observed in these systems. The common feature of these reactions is that k_d does not depend on the pH in the 6.0 – 13.0 range. In contrast, a definite pH dependence was observed during the decomposition of *N*-chloro-BCAAs, i.e. in the absence of the *N*-methyl substituent.[7] It was also established that the kinetic features are not affected by the excess of *N*-methyl amino acids. The rate constant of the

decomposition decreases by increasing the bulkiness of the alkyl chain on the α-carbon indicating the importance of steric effects (Table 2). The data also implies that the differences in the electron donating inductive effect of the α-alkyl chain do not affect significantly the rates of these reactions.

Table 2. Rate constants for the decomposition of *N*-chloro-*N*-methyl amino acids. I = 1.00 M ($NaClO_4$), T = 25.0 °C

Amino acid	$k_d \times 10^2$ (s^{-1})	Ref.
N-chloro-*N*-methylalanine	9.60 ± 0.29	this work
N-chloro α-alanine	0.0295	24
N-chloro-*N*-methylleucine	2.27 ± 0.13	this work
N-chloro leucine	0.0383	7
N-chloro-*N*-methylisoleucine	1.63 ± 0.02	this work
N-chloro isoleucine	0.0228	7
N-chloro-*N*-methylvaline	1.11 ± 0.06	this work
N-chloro valine	0.0196	7
N-chloro-*N*-methyglycine	0.010 ± 0.003	this work
N-chloro glycine[a]	NA	23

a: Only the OH^- assisted path is operative.[23]

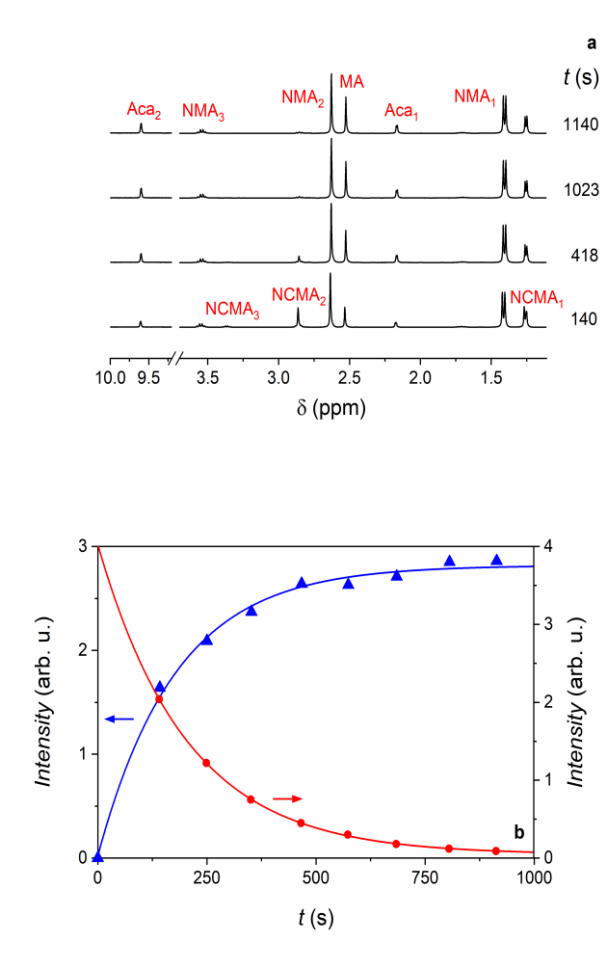

Figure 3. ^{1}H NMR results obtained by monitoring the decomposition of NCMA under neutral conditions, a: the spectra and b: the intensities of the ^{1}H NMR peaks of $NCMA_2$ (● 2.86 ppm) and MA (▲ 2.53 ppm) as a function of time (markers) and the fitted curves using first order rate equation (solid lines). $c_{NMA}{}^{0} = 3.00 \times 10^{-3}$ M, $c_{NCMA}{}^{0} = 3.00 \times 10^{-3}$ M, pH = 7.31, $T = 25.0$ °C.

^{1}H NMR measurements were carried out to identify the intermediates and products as well as to monitor their concentration profiles. The assignments of the peaks for all systems are listed in Table S1. As an example, time resolved NMR spectra for the decomposition of NCMA are shown in Figure 3a. As expected, the intensities of the characteristic peaks of NMA do not change as a function of time. The NCMA peaks diminish and new peaks assigned to acetaldehyde and methylamine emerge. The intensities as a function of time correspond to a first

order process (Figure 3b). The NMR results in the NCMA, NCML, NCMI and NCMV systems are fully analogous. In each case, the characteristic -CHO peak in the 9.55 – 9.60 ppm region, and the new aliphatic CH peaks are consistent with the formation of the corresponding aldehyde under neutral conditions.

The first order rate constants obtained from the spectrophotometric and NMR measurements are in good agreement in each system, although the experimental conditions were somewhat different because constant ionic strength was not set in the NMR experiments. Only one rate determining step is operative in the decomposition processes and the overall stoichiometry is given by Eq. (5).

$$ClN(CH_3)-CH(R)-COO^- + H_2O = R-CHO + Cl^- + CH_3NH_2 + CO_2 \quad (5)$$

Upon increasing the pH, the characteristic peaks of the aldehydes become wider and eventually disappear from the NMR spectra of the spent reaction mixtures as shown for NCMI in Figure 4. These observations are interpreted by considering the keto – enol tautomeric and hydration equilibria of the aldehydes (Scheme S1). The CH peaks of the diol and the enol forms are not seen in the NMR spectra because they are under the suppressed water signal. At high pH, the geminal diol and also the enol form undergo deprotonation. The tautomerization and the hydration equilibria of the aldehydes are base catalyzed.[49, 50] The conversion of the different isomers into each other leads to substantial line broadening when the pH is increased.

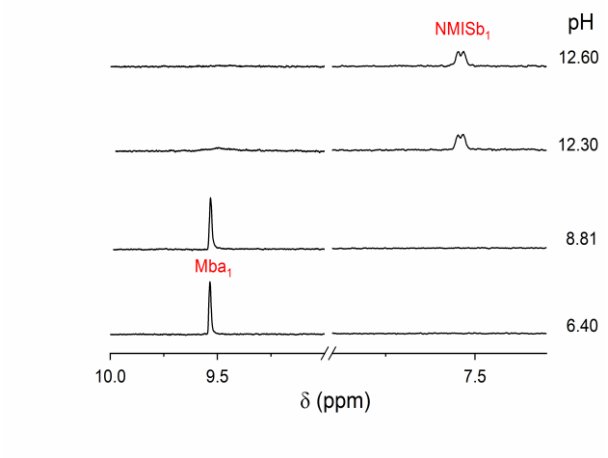

Figure 4. ^{1}H NMR spectra of the spent reaction mixture as a function of pH in the decomposition of NCMI. $c_{NMI}^{0} = 3.00 \times 10^{-3}$ M, $c_{NCMI}^{0} = 3.00 \times 10^{-3}$ M, $T = 25.0$ °C.

A new set of peaks also appears at ~7.6 ppm (Figure 4) and in the aliphatic spectral region (Figure S4). The intensities of theses peaks increase upon increasing the pH. The observations confirm the formation of a Schiff base from aldehyde and methylamine which are the final products of the decomposition reaction under neutral conditions. This was demonstrated by reacting aldehydes with methylamine in separate NMR experiments (Figure S5). When the pH is increased, the aldehyde peaks disappear, the methylamine peak shifts upfield and its intensity becomes smaller. Simultaneously, the characteristic peaks of the Schiff base emerge. When the pH of the spent alkaline reaction mixtures set to neutral, methylamine becomes fully protonated (pK_a = 10.96)[51] and the Schiff base formation equilibrium is shifted backward. Consequently, the Schiff base peaks are absent in the NMR spectra and the peaks of acetaldehyde appear again.

Since the formation of the Schiff bases is fast, monitoring their NMR peaks as a function of time offers a convenient way to follow the decomposition kinetics of the corresponding alkyl substituted *N*-chloro-*N*-methyl amino acids under alkaline conditions (Figure S6). Again, the rate constants obtained from spectrophotometric and NMR measurements are in excellent agreement.

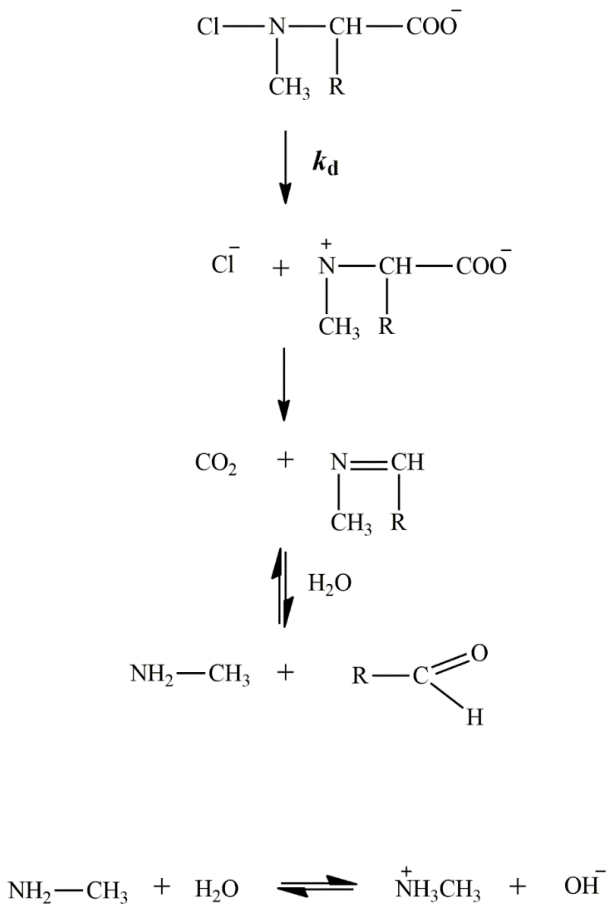

Scheme 1. The common kinetic model for the decomposition of NCMG (only under neutral conditions), NCMA, NCML, NCMI and NCMV.

The decomposition reactions of the *N*-chloro-*N*-methyl alkyl substituted amino acids can be interpreted in terms of a common mechanism (Scheme 1) which improves the earlier proposed fragmentation model.[39] The rates of the decomposition of *N*-chloro alanine and BCAAs show a linear dependence on [OH^-] which is consistent with the formation of a carbanion in the rate determining step. In contrast, the OH^- assisted reaction path is not operative in the degradation of NCMA, NCML, NCMI and NCMV. Supposedly, the *N*-methyl group increases the basicity of the α-carbon atom significantly and makes the formation of a carbanion less favorable. In addition, the combined electron donating effect of the *N*-methyl and the α-alkyl groups enhances

the spontaneous elimination of Cl^-. For this reason, the *N*-chlorinated *N*-methyl substituted amino acids decompose considerably faster than their non-substituted analogues. Subsequent decarboxylation yields an imine (Schiff base) which is converted into the final products through an equilibrium hydration step.

Typical time resolved spectra for the decomposition of NCMG are consistent with a simple first-order decomposition process in the entire neutral – alkaline pH range (Figure S7). However, a clear induction period is observed in the kinetic traces at lower wavelength under alkaline conditions (Figure 5).

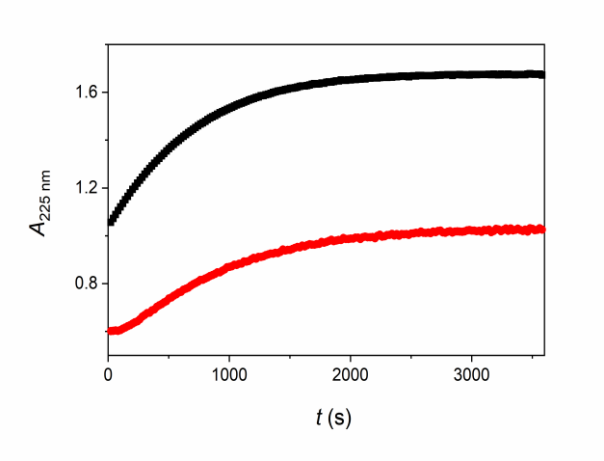

Figure 5. Kinetic trace exhibiting an induction period during the decomposition of NCMG (red line). The induction period is suppressed by adding glyoxylate ion to the reaction mixture initially (black line). $c_{NMG}^0 = 3.00 \times 10^{-3}$ M, $c_{NCMG}^0 = 3.00 \times 10^{-3}$ M, $c_{Gl}^0 = 3.00 \times 10^{-3}$ M, $[OH^-] = 5.00 \times 10^{-2}$ M, $T = 25.0$ °C.

The rate constant of the decomposition, k_d^{obs}, is a linear function of $[OH^-]$ with non-zero intercept (Figure S8).

$$k_d^{obs} = k_d + k_d^{OH}[OH^-] \quad (6)$$

Evaluation of the data yields $k_d = (1.04 \pm 0.26) \times 10^{-4}$ s^{-1} and $k_d^{OH} = (2.07 \pm 0.08) \times 10^{-2}$ M^{-1} s^{-1}. k_d is considerably smaller than the rate constants obtained in the other systems (Table 2). This

is most likely the consequence of the absence of an electron donating alkyl group on the α-carbon atom in NCMG. The value of k_d agrees well with the result reported earlier.[39]

The two-term rate expression confirms that the decomposition occurs via two competing reaction paths. According to ^{1}H NMR experiments, one of the products is methylamine regardless of the pH. If the reaction follows similar pattern than the decomposition of MCA[24], the other product should be formaldehyde and glyoxylate ion in the neutral and the alkaline pH range, respectively. The characteristic CHO peaks are not seen in the ^{1}H NMR spectra of the spent reaction mixture and direct identification of the oxo products is not feasible. This is most likely the consequence of the fast hydration and keto – enol tautomerization equilibria of these compounds (Scheme S1). It is also possible that the water signal overlaps the NMR peaks of the dominant forms, thus, they are undetectable.

Similarly to the other systems, the ^{1}H NMR spectra reveal the formation of a Schiff base with characteristic peaks at 3.34 and 7.72 ppm at high pH (Figure 6a). The kinetic traces from the NMR and spectrophotometric measurements are fully consistent with each other (Figure 6b), and the rate constants obtained by the two methods agree reasonably well.

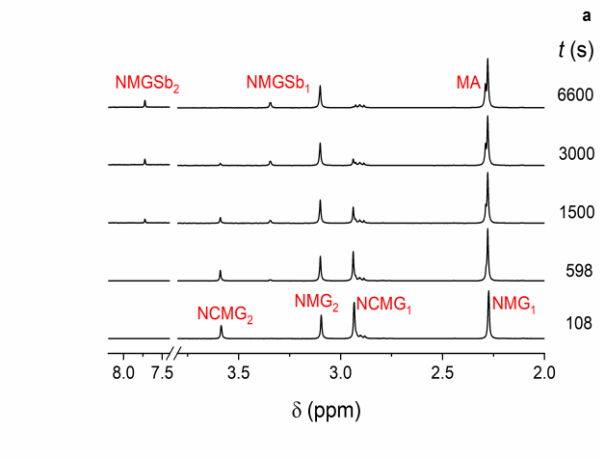

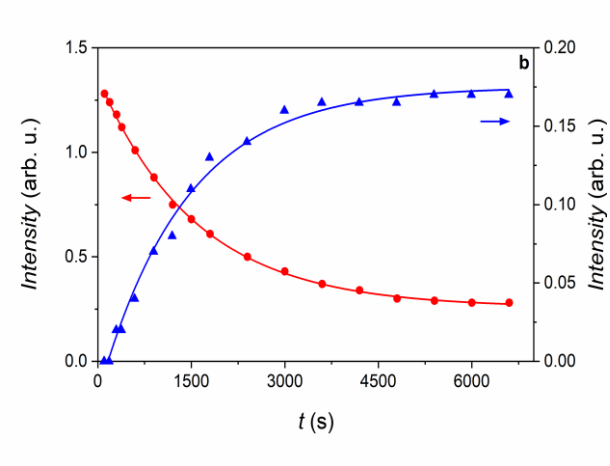

Figure 6. ^{1}H NMR results for the decomposition of NCMG under alkaline conditions, a: the spectra and b: the intensities of the ^{1}H NMR peaks of $NCMG_1$ (● 2.91 ppm) and $NMGSb_1$ (▲ 3.34 ppm) as a function of time and fitted curves using a first order rate equation (solid lines). $c_{NMG}^{0} = 3.00 \times 10^{-3}$ M, $c_{NCMG}^{0} = 3.00 \times 10^{-3}$ M, $[OH^-] = 5.00 \times 10^{-2}$ M, $T = 25.0$ °C.

Quite fortuitously, the Schiff base formation makes possible to identify the oxo compound formed. In separate experiments, it was confirmed that the formation of a Schiff base from methylamine and formaldehyde is not detectable under the conditions applied. This is most likely due to the coupled hydration equilibrium (Scheme S1) which practically eliminates the oxo form of formaldehyde. Consequently, the corresponding Schiff base formation equilibrium is shifted completely toward the dissociation. At the same time, the noted peaks are present in the NMR spectrum of the reaction mixture of methylamine and glyoxylate ion, i.e. the Schiff base is formed from these compounds as shown in Eq. (7). In a set of separate experiments, this equilibrium was studied in more detail (cf. SI and Figure S9).

$$CH_3NH_2 + CHO{-}COO^- \rightleftharpoons CH_3N{=}CH{-}COO^- + H_2O \qquad (7)$$

It is a rational assumption that the decomposition of NCMG proceeds according to Scheme 1 and produces formaldehyde under neutral conditions.

As it was suggested before[7, 23, 24], the OH^- assisted reaction path is initiated by the formation of a carbanion in an equilibrium step (K_{OH}), which is followed by the dechlorination in a rate determining step (k_1), $k_d^{OH} = K_{OH}\, k_1$ (Scheme S2). In the next reaction sequence, the equilibrium is rapidly established between the Schiff base and the final products. On the 0basis of this model, the noted induction period in the kinetic traces at lower wavelengths (Figure 5) can be interpreted by considering that the Schiff base has considerable contribution to the absorbance under 250 nm. This compound is not detectable at the beginning of the decomposition because the corresponding equilibrium (Eq. (7)) is completely shifted to the left. As the decomposition proceeds, the equilibrium concentration of the Schiff base increases and eventually becomes detectable. In agreement with these considerations, the induction period is suppressed by initially adding glyoxylate ion to the reaction mixture (Figure 5). Model calculations on the basis of a simplified kinetic model confirm these kinetic features (cf. SI and Figure S10).

The *N*-chloro-*N*-methyl amino acids decompose close to two orders of magnitude faster compared to the non-substituted parent compounds which is due to the *N*-methyl group. The degradation follows the same kinetic pattern, i.e. the rate of these reactions does not depend on the pH and the same final product is formed in the entire pH range. The only exception is *N*-chloro sarcosine which decomposes via two parallel reaction paths leading to different final products. This distinct behavior is most likely due to the lack of an alkyl substituent on the α-carbon atom. The results reveal that the lifetimes of the *N*-chloro-*N*-methyl amino acids are relatively short, only a few minutes. At physiological pH, the decomposition of these compounds yields methylamine and aldehydes which are not particularly toxic. However, they are frequently implicated as the source of taste and odor issues in drinking water treatment technologies.

ACKNOWLEDGEMENTS

The research was supported by the EU and co-financed by the European Regional Development Fund under the project GINOP-2.3.2-15-2016-00008, by the Hungarian Science Foundation (OTKA K124983), as well as by the ÚNKP-19-3 New National Excellence Program of the Ministry of Human Capacities. F.S. is indebted to the Gedeon Richter's Talentum Fundation for financial support.

Supporting Information

The Supporting Information is available free of charge at https://pubs.acs.org …...

Table S1, The assignments of the ^{1}H NMR peaks.; Figure S1, The concentration dependence of k_{obs}^{1st}; Figure S2, The temperature dependence of k_{obs}^{2nd}; Figure S3, Kinetic trace recorded during the decomposition of NCMA,; Figure S4, ^{1}H NMR spectra of the spent reaction mixtures in the NCMI system. Figure S5, ^{1}H NMR results obtained in the acetaldehyde – methylamine system.; Figure S6, ^{1}H NMR results obtained by monitoring the decomposition of NCMA.; Figure S7, Spectral changes during the decomposition of NCMG.; Figure S8, The rate constant of the decomposition of NCMG as a function of [OH^{-}]. Scheme S1, The keto – enol tautomerism and hydration equilibria of the aldehydes.; Scheme S2, Mechanisms for the decomposition of NCMG.; The discussion of the Schiff base formation equilibrium between methylamine and glyoxylate ion.; Kinetic modelling of the decomposition of NCMG.

REFERENCES

(1) Ram, N. M. (1985) A review of the significance and formation of chlorinated N-organic compounds in water supplies including preliminary studies on the chlorination of alanine, tryptophan, tyrosine, cytosine, and syringic acid. *Environment International 11*, 441-451.

(2) van Veldhoven, K., Keski-Rahkonen, P., Barupal, D. K., Villanueva, C. M., Font-Ribera, L., Scalbert, A., Bodinier, B., Grimalt, J. O., Zwiener, C., Vlaanderen, J., Portengen, L.,

Vermeulen, R., Vineis, P., Chadeau-Hyam, M., and Kogevinas, M. (2018) Effects of exposure to water disinfection by-products in a swimming pool: A metabolome-wide association study. *Environment International 111*, 60-70.
(3) Tsamba, L., Correc, O., and Couzinet, A. (2020) +Chlorination by-products in indoor swimming pools: Development of a pilot pool unit and impact of operating parameters. *Environment International 137*, 105566.
(4) White, G. C. (1992) *Handbook of Chlorination and Alternative Disinfectants*. Van Nostrand Reinhold, New York.
(5) Trogolo, D., and Arey, J. S. (2017) Equilibria and Speciation of Chloramines, Bromamines, and Bromochloramines in Water. *Environmental Science & Technology 51*, 128-140.
(6) Amiri, F., Mesquita, M. M. F., and Andrews, S. A. (2010) Disinfection effectiveness of organic chloramines, investigating the effect of pH. *Water Research 44*, 845-853.
(7) Szabó, M., Bíró, V., Simon, F., and Fábián, I. (2020) The decomposition of N-chloro amino acids of essential branched-chain amino acids: Kinetics and mechanism. *Journal of Hazardous Materials 382*, 120988.
(8) Hrudey, S. E., Gac, A., and Daignault, S. A. (1988) Potent Odour-Causing Chemicals Arising from Drinking Water Disinfection. *Water Science and Technology 20*, 55-61.
(9) Daignault, S. A., Gac, A., and Hrudey, S. E. (1988) Analysis of low molecular weight aldehydes causing odour in drinking water. *Environmental Technology Letters 9*, 583-588.
(10) Armesto, X. L., Canle, M., Garcia, M. V., and Santaballa, J. A. (1998) Aqueous chemistry of N-halo-compounds. *Chemical Society Reviews 27*, 453-460.
(11) Kettle, A. J., and Winterbourn, C. C. (1997) Myeloperoxidase: A key regulator of neutrophil oxidant production. *Redox Report 3*, 3-15.
(12) Sicking, W., Somnitz, H., and Schmuck, C. (2012) DFT Calculations Suggest a New Type of Self-Protection and Self-Inhibition Mechanism in the Mammalian Heme Enzyme Myeloperoxidase: Nucleophilic Addition of a Functional Water rather than One-Electron Reduction. *Chemistry - A European Journal 18*, 10937-10948.
(13) Hawkins, C. L., and Davies, M. J. (1999) Hypochlorite-induced oxidation of proteins in plasma: formation of chloramines and nitrogen-centred radicals and their role in protein fragmentation. *Biochemical Journal 340*, 539.
(14) Hawkins, C. L., and Davies, M. J. (2000) Hypochlorite-induced damage to red blood cells: evidence for the formation of nitrogen-centred radicals. *Redox Report 5*, 57-59.
(15) Hawkins, C. L., and Davies, M. J. (2001) Hypochlorite-induced damage to nucleosides: Formation of chloramines and nitrogen-centered radicals. *Chemical Research in Toxicology 14*, 1071-1081.
(16) Hawkins, C. L., and Davies, M. J. (2002) Hypochlorite-induced damage to DNA, RNA, and polynucleotides: Formation of chloramines and nitrogen-centered radicals. *Chemical Research in Toxicology 15*, 83-92.
(17) Davies, M. J., and Hawkins, C. L. (2001) Hypochlorite-induced damage to DNA, RNA and polynucleosides: Formation of chloramines and nitrogen-centered radicals. *Free Radical Biology and Medicine 31*, S85-S85.
(18) Pullar, J. M., Winterbourn, C. C., and Vissers, M. C. M. (2002) The effect of hypochlorous acid on the expression of adhesion molecules and activation of NF-kappa B in cultured human endothelial cells. *Antioxidants and Redox Signaling 4*, 5-15.

(19) King, D. A., Hannum, D. M., Qi, H. S., and Hurst, J. K. (2004) HOCI-mediated cell death and metabolic dysfunction in the yeast Saccharomyces cerevisiae. *Archives of Biochemistry and Biophysics 423*, 170-181.
(20) Mazzio, E. A., Reams, R. R., and Soliman, K. F. A. (2004) The role of oxidative stress, impaired glycolysis and mitochondrial respiratory redox failure in the cytotoxic effects of 6-hydroxydopamine in vitro. *Brain Research 1004*, 29-44.
(21) Stanley, N. R., Pattison, D. I., and Hawkins, C. L. (2010) Ability of Hypochlorous Acid and N-Chloramines to Chlorinate DNA and Its Constituents. *Chemical Research in Toxicology 23*, 1293-1302.
(22) Szabó, M., Simon, F., and Fábián, I. (2019) The formation of N-chloramines with proteinogenic amino acids. *Water Res 165*, 114994.
(23) Szabó, M., Baranyai, Z., Somsák, L., and Fábián, I. (2015) Decomposition of N-Chloroglycine in Alkaline Aqueous Solution: Kinetics and Mechanism. *Chemical Research in Toxicology 28*, 1282-1291.
(24) Simon, F., Szabó, M., and Fábián, I. (2019) pH controlled byproduct formation in aqueous decomposition of N-chloro-α-alanine. *Journal of Hazardous Materials 362*, 286-293.
(25) Fehér, P. P., Purgel, M., Lengyel, A., Stirling, A., and Fábián, I. (2019) The mechanism of monochloramine disproportionation under acidic conditions. *Dalton Transactions 48*, 16713-16721.
(26) Del Rizzo, P. A., Krishnan, S., and Trievel, R. C. (2012) Crystal Structure and Functional Analysis of JMJD5 Indicate an Alternate Specificity and Function. *Molecular and Cellular Biology 32*, 4044-4052.
(27) Hagos, Y., Schley, G., Schoedel, J., Krick, W., Burckhardt, G., Willam, C., and Burckhardt, B. C. (2012) alpha-Ketoglutarate-related inhibitors of HIF prolyl hydroxylases are substrates of renal organic anion transporters 1 (OAT1) and 4 (OAT4). *Pflugers Archiv-European Journal of Physiology 464*, 367-374.
(28) Kalliri, E., Grzyska, P. K., and Hausinger, R. P. (2005) Kinetic and spectroscopic investigation of Co-II, Ni-II, and N-oxalylglycine inhibition of the Fe-II/alpha-ketoglutarate dioxygenase, TauD. *Biochemical and Biophysical Research Communications 338*, 191-197.
(29) Bojarova, P., and Williams, S. J. (2008) Sulfotransferases, sulfatases and formylglycine-generating enzymes: a sulfation fascination. *Current Opinion in Chemical Biology 12*, 573-581.
(30) Frese, M.-A., and Dierks, T. (2009) Formylglycine Aldehyde Tag-Protein Engineering through a Novel Post-translational Modification. *Chembiochem 10*, 425-427.
(31) Prechoux, A., Genicot, S., Rogniaux, H., and Helbert, W. (2013) Controlling Carrageenan Structure Using a Novel Formylglycine-Dependent Sulfatase, an Endo-4S-iota-Carrageenan Sulfatase. *Marine Biotechnology 15*, 265-274.
(32) Riano, V. M., and Rademann, J. (2012) Formylglycine-peptides for the identification of novel pTyr mimetics through a fragment based dynamic ligation screening (DLS) approach. *Journal of Peptide Science 18*, S72-S72.
(33) Zhao, H., Zhou, Y., Han, C., Liu, Y. D., and Zhong, R. (2020) Degradation Mechanisms and Substituent Effects of N-Chloro-α-Amino Acids: A Computational Study. *Environmental Science & Technology 54*, 2635-2645.
(34) Moolenaar, S. H., Poggi-Bach, J., Engelke, U. F. H., Corstiaensen, J. M. B., Heerschap, A., de Jong, J. G. N., Binzak, B. A., Vockley, J., and Wevers, R. A. (1999) Defect in

Dimethylglycine Dehydrogenase, a New Inborn Error of Metabolism: NMR Spectroscopy Study. *Clinical Chemistry 45*, 459.
(35) Meissner, T., and Mayatepek, E. (1997) Sarcosinaemia in a patient with severe progressive neurological damage and hypertrophic cardiomyopathy. *Journal of Inherited Metabolic Disease 20*, 717-718.
(36) Gerritsen, T., and Waisman, H. A. (1966) Hypersarcosinemia. *New England Journal of Medicine 275*, 66-69.
(37) Kang, E. S., Seyer, J., Todd, T. A., and Herrera, C. (1983) Variability in the phenotypic expression of abnormal sarcosine metabolism in a family. *Human Genetics 64*, 80-85.
(38) Sreekumar, A., Poisson, L. M., Rajendiran, T. M., Khan, A. P., Cao, Q., Yu, J., Laxman, B., Mehra, R., Lonigro, R. J., Li, Y., Nyati, M. K., Ahsan, A., Kalyana-Sundaram, S., Han, B., Cao, X., Byun, J., Omenn, G. S., Ghosh, D., Pennathur, S., Alexander, D. C., Berger, A., Shuster, J. R., Wei, J. T., Varambally, S., Beecher, C., and Chinnaiyan, A. M. (2009) Metabolomic profiles delineate potential role for sarcosine in prostate cancer progression. *Nature 457*, 910-914.
(39) Armesto, X. L., Canle L, M., Losada, M., and Santaballa, J. A. (1994) Concerted Grob Fragmentation in N-Halo-.alpha.-amino Acid Decomposition. *The Journal of Organic Chemistry 59*, 4659-4664.
(40) Adam, L. C., Fábián, I., Suzuki, K., and Gordon, G. (1992) Hypochlorous acid decomposition in the pH 5-8 region. *Inorganic Chemistry 31*, 3534-3541.
(41) Peintler, G., Nagypal, I., and Epstein, I. R. (1990) Systematic design of chemical oscillators. 60. Kinetics and mechanism of the reaction between chlorite ion and hypochlorous acid. *J. Phys. Chem. 94*, 2954-2958.
(42) Fábián, I., and Gordon, G. (1991) Complex- formation reactions of the chlorite ion. *Inorganic Chemistry 30*, 3785-3787.
(43) Irving, H. M., Miles, M. G., and Pettit, D. L. (1967) A study of some problems in determining the stoicheiometric proton dissociation constants of complexes by potentiometric titrations using a glass electrode. *Analytica Chimica Acta 38*, 475-488.
(44) Gans, P., Sabatini, A., and Vacca, A. (1985) SUPERQUAD: an improved general program for computation of formation constants from potentiometric data. *Journal of the Chemical Society, Dalton Transactions*, 1195-1200.
(45) Fábián, I., and Lente, G. (2010) Light-induced multistep redox reactions: The diode-array spectrophotometer as a photoreactor. *Pure and Applied Chemistry 82*, 1957-1973.
(46) (2018) OriginPro 2018b, Microcal Software Inc., Northampton, MA.
(47) Hypochlorous acid and amino acids exist as an equilibrium mixture of various protonated forms in aqueous solution. The concentration ratios of these species are dependent on the pH. Distinction between the different forms is made only when it is required by the clarity of presentation.
(48) Qiang, Z., and Adams, C. D. (2004) Determination of Monochloramine Formation Rate Constants with Stopped-Flow Spectrophotometry. *Environmental Science & Technology 38*, 1435-1444.
(49) Pocker, Y., and Dickerson, D. G. (1969) Hydration of propionaldehyde, isobutyraldehyde, and pivalaldehyde. Thermodynamic parameters, buffer catalysis and transition state characterization. *The Journal of Physical Chemistry 73*, 4005-4012.
(50) Green, L. R., and Hine, J. (1973) Isobutyraldehyde. Kinetics of acid and base-catalyzed equilibrations in water. *The Journal of Organic Chemistry 38*, 2801-2806.

(51) Debreczeni, F., and Nagypál, I. (1983) NMR relaxation studies in solutions of transition metal complexes. IX. Dynamics of equilibria in aqueous solutions of some copper(II) - nitrilotriacetate–B ligand mixed ligand complexes. *Inorganica Chimica Acta 72*, 61-65.

Table of Contents Art